JACS
JOURNAL OF THE AMERICAN CHEMICAL SOCIETY
Article
pubs.acs.org/JACS

# Two-Photon Absorbing Dyes with Minimal Autofluorescence in Tissue Imaging: Application to *in Vivo* Imaging of Amyloid-$\beta$ Plaques with a Negligible Background Signal

Dokyoung Kim,[†,∥] Hyunsoo Moon,[†,∥] Sung Hoon Baik,[‡,∥] Subhankar Singha,[†,∥] Yong Woong Jun,[†] Taejun Wang,[§] Ki Hean Kim,*[,§] Byung Sun Park,[⊥] Junyang Jung,[⊥] Inhee Mook-Jung,*[,‡] and Kyo Han Ahn*[,†]

[†]Department of Chemistry, Center for Electro-Photo Behaviors in Advanced Molecular Systems, Pohang University of Science and Technology (POSTECH), 77 Cheongam-Ro, Nam-Gu, Pohang, Gyungbuk 790-784, Republic of Korea

[‡]Department of Biochemistry and Biomedical Sciences, College of Medicine, Seoul National University, 103 Daehak-Ro, Jongro-Gu, Seoul 110-799, Republic of Korea

[§]Division of Integrative Biosciences and Biotechnology, Pohang University of Science and Technology (POSTECH), 77 Cheongam-Ro, Nam-Gu, Pohang, Gyungbuk 790-784, Republic of Korea

[⊥]Department of Anatomy and Neurobiology, School of Medicine, Biomedical Science Institute, Kyung Hee University, 26 Kyungheedae-Ro, Dongdaemun-Gu, Seoul 130-701, Republic of Korea

Supporting Information

**ABSTRACT:** Fluorescence imaging of tissues offer an essential means for studying biological systems. Autofluorescence becomes a serious issue in tissue imaging under excitation at UV–vis wavelengths where biological molecules compete with the fluorophore. To address this critical issue, a novel class of fluorophores that can be excited at ~900 nm under two-photon excitation conditions and emits in the red wavelength region (≥600 nm) has been disclosed. The new $\pi$-extended dipolar dye system shows several advantageous features including minimal autofluorescence in tissue imaging and pronounced solvent-sensitive emission behavior, compared with a widely used two-photon absorbing dye, acedan. As an important application of the new dye system, one of the dyes was developed into a fluorescent probe for amyloid-$\beta$ plaques, a key biomarker of Alzheimer's disease. The probe enabled *in vivo* imaging of amyloid-$\beta$ plaques in a disease-model mouse, with negligible background signal. The new dye system has great potential for the development of other types of two-photon fluorescent probes and tags for imaging of tissues with minimal autofluorescence.

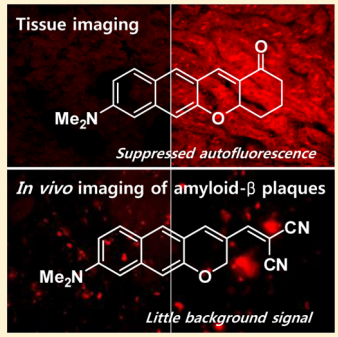


## INTRODUCTION

The detection and imaging of biomolecules are essential for studying biological progresses in living systems. To this end, the fluorescence method combined with an appropriate molecular probe has provided a versatile tool as it enables operationally simple, cost-effective, noninvasive, highly sensitive detection and visualization of organisms at a subcellular level.[1] Accordingly, many fluorescent probes have been developed for the detection and imaging of various analytes.

During the last two decades, two-photon microscopy (TPM) based on nonlinear interaction between light and matter has emerged as an important tool for imaging of biological tissues where light scattering becomes a serious issue under the conventional one-photon confocal microscopy (OPM). The probability of two-photon excitation diminishes dramatically outside the focal point, a distinct feature from the one-photon excitation, and the focal point is scanned throughout a tissue region of interest to offer 3D images with an exceptionally high resolution. Furthermore, excitation at near-infrared (NIR) wavelengths of the first biological optical window (650–950 nm) allows for deeper penetration (down to 1000 $\mu$m) and minimal absorption through highly scattering tissue media, with suppressed photodamage and photobleaching to tissues.[2] These promising features of TPM have motivated chemists in search for two-photon absorbing dyes with desirable photophysical properties and the corresponding molecular probes for the detection and imaging of biological analytes in tissues of living systems.[3]

Acedan, 6-acetyl-2-(dimethylamino)naphthalene, and its derivatives constitute one of important classes of nonsymmetric donor–acceptor (D–A) type dyes with sufficient two-photon absorption properties for bioimaging applications (Scheme 1).[4] Acedan is structurally simple and thus easy to modify, making it a typical two-photon dye in the development of various fluorescent probes for biomolecules and organelles in recent years.[5,3e] During our own journey in this endeavor,[6,4b] we have recognized that, in spite of those novel features, acedan and

Received: January 18, 2015
Published: May 7, 2015





DOI: 10.1021/jacs.5b03548
J. Am. Chem. Soc. 2015, 137, 6781–6789

**Scheme 1. Structures of Acedan, Acylic $\pi$-Extended Analogues, and New Dyes 1−4**

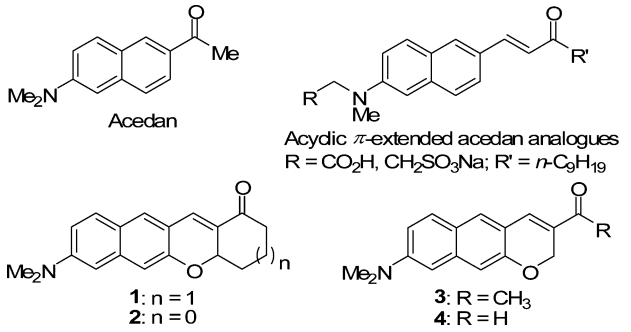


related two-photon dyes pose a drawback in tissue imaging. Acedan has the maximum absorption and emission wavelengths in the rather shorter wavelength region ($\lambda_{abs}$ = 364 nm and $\lambda_{em}$ = 484 nm in ethanol). Hence, two-photon excitation of acedan and its analogues in the wavelength range of 740−780 nm and collection of emission light in the green wavelength region (around 484 nm) cause significant undesired autofluorescence from intrinsic biomolecules in the course of tissue imaging (see below). The intrinsic biomolecules present in the tissues such as NADH, riboflavins, retinol, folic acid, etc. are responsible for the autofluorescence (due to two-photon absorption and the emission in the green region).[7] Accordingly, acedan derivatives are excited with a low-power laser and the emission is collected at a narrow band to reduce the autofluorescence and reabsorption of the emitted light by the biomolecules. However, even under usual tissue imaging conditions (5−10 mW at the focal point), still notable autofluorescence is significant when acedan is used for imaging of tissue samples prepared under usual fixitive conditions (see below). Use of a lower laser power for the two-photon excitation, on the other hand, limits the light penetration to a rather shallow depth (<300 $\mu$m).[7d] We reasoned that two-photon absorbing dyes that absorb and emit light at the longer wavelengths (two-photon excitation around 900 nm and emission above 600 nm) would alleviate the autofluorescence caused by using dyes with the shorter absorption and emission wavelengths, because intrinsic biomolecules show a minium two-photon absorption cross-section value when excited around 900 nm and also most of them do not emit in the red wavelength region.[7a] In addition, use of a longer wavelength is an effective way to enhance the imaging depth as the serious light scattering is dramatically reduced as the excitation wavelength increases.[8,2i]

Here, we wish to disclose a new dipolar dye system that shows promising two-photon imaging properties, in particular, greatly suppressed autofluorescence in fluorescence imaging of tissues. Furthermore, we have applied one of the dyes to develop a two-photon probe for *in vivo* imaging of amyloid-$\beta$ plaques in the brain of an Alzheimer's disease mouse model with a negligible background signal, addressing a common drawback observed with existing probes.

## RESULTS AND DISCUSSION

**Novel Two-Photon Absorbing Dyes with Suppressed Autofluorescence in Tissue Imaging.** The designed dipolar dye system, which may be classified to be $\pi$-extended acedan analogues (**1**−**4**), consists of a tri- or a tetracyclic ring with an additional carbon−carbon double bond inserted between the naphthalene ring and acetyl group of acedan in such a way that the double bond is conformationally locked in the *trans* form (Scheme 1).

A few acyclic analogues of such $\pi$-extended dyes are known,[9] but they are expected to show weaker emission owing to the free rotation of the $\pi$-extended moiety, in addition to be chemically and photochemically less stable. All the new dyes can be readily synthesized from a common intermidiate, 6-(dimethylamino)-3-hydroxy-2-naphthaldehyde (**7**) previously reported by us (Scheme 2).[10] Introduction of the enone moiety

**Scheme 2. Synthesis of $\pi$-Extended Acedan Derivatives 1−4**[a]

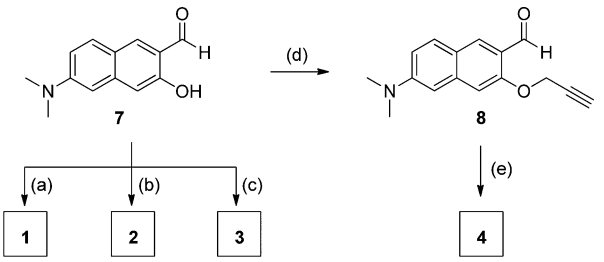


[a]Reagent and conditions: (a) 2-cyclohexen-1-one, DABCO, water−1,4-dioxane (1:2, v/v), sonication, 45−50 °C, 48 h, 38%; (b) 2-cyclopenten-1-one, DABCO, water−1,4-dioxane (1:1, v/v), sonication, 45−50 °C, 48 h, 22%; (c) 3-buten-2-one, $MgI_2$, TMEDA, DMAP, MeOH, 25 °C, 24 h, 28%; (d) propargyl bromide, $K_2CO_3$, DMF, 25 °C, 12 h, 100%; (e) CuI, $CH_3CN$, 82 °C, 71%.

enclosed in the new ring could be performed by the Baylis−Hillman reaction to directly produce dyes **1**−**3**.[11] Dye **4** can be prepared in a different route involving Cu(I)-catalyzed cyclization of an *o*-formylaryl propargyl ether (**8**),[12] which can be generated from naphthaldehyde **7**. Details of the syntheses and characterization data of the new compounds are given in the Experimental Section.

Dyes **1**−**4** indeed have the absorption and emission bands at substantially longer wavelengths ($\lambda_{abs}$ = 398−427 nm and $\lambda_{em}$ = 546−617 nm in ethanol) than those of acedan (Figure 1 and

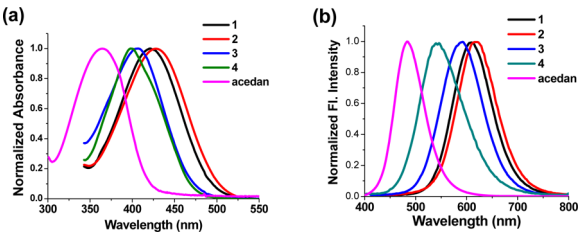


**Figure 1.** (a) Normalized UV−vis absorption and (b) normalized fluorescence emission spectra of **1**−**4** and acedan. The fluorescence emission spectra were measured under excitation at the maximum absorption wavelength of each compound (10 $\mu$M in ethanol) at 25 °C.

Table 1). Importantly, dyes **1** and **2** can be excited at ~900 nm, an optimum wavelength for tissue imaging in the first optical window[13] under two-photon excitation conditions, and emit in the red wavelength region. Acedan can be excited at best at around 780 nm (Figure 1a) and emits in the green region where intrinsic biomolecules such as NADH, ribioflavins also emit.[14]

Although the fluorescence intensity of the new dyes is a little lower than that of acedan in a given solvent (Table 1, Supporting Information Figures S1 and S3), they are expected


DOI: 10.1021/jacs.5b03548
J. Am. Chem. Soc. 2015, 137, 6781−6789

**Table 1. Photophysical Properties of Compounds 1−4 and Acedan.**[a]

| comp. | $\lambda_{abs}$ | $\varepsilon^b$ | $\lambda_{em}{}^c$ | $\Phi_F{}^d$ | $\Phi_F{}^e$ | $\Phi_F{}^f$ | log $P^g$ |
|---|---|---|---|---|---|---|---|
| **1** | 421 | 13,000 | 609 | 0.42 | 0.32 | 0.12 | 4.08 |
| **2** | 427 | 14,300 | 617 | 0.37 | 0.26 | 0.08 | 3.51 |
| **3** | 407 | 11,500 | 592 | 0.47 | 0.34 | 0.14 | 3.77 |
| **4** | 398 | 15,500 | 546 | 0.44 | 0.37 | 0.06 | 3.72 |
| Acedan | 364 | 10,700 | 484 | 0.72 | 0.56 | (0.52) | 3.00 |

[a]All the measurements were carried out at 25 °C with the compounds (10 $\mu$M) dissolved in ethanol. [b]L mol$^{-1}$ cm$^{-1}$. [c]Measured under excitation at the maximum absorption wavelength in the given solvent. [d−f]The fluorescence quantum yields ([d]$CH_2Cl_2$, [e]$CH_3CN$, [f]EtOH) were determined using acedan as a reference dye ($\Phi_F$ = 0.52 in ethanol).[17] [g]Log *P* values were calculated using ACDLab-ACDLog *P* software.

to give high-contrasting TPM images of tissues because of reduced autofluorescence from the intrinsic fluorophores.[7] The absorption and emission wavelengths of donor−acceptor (D−A) type dyes such as acedans and its analogues are in general sensitive to the environment because they form the intramolecular charge-transfer (ICT) excited states; they emit at the longer wavelength as the solvent polarity increases.[15] Also, such D−A type dyes usually show strong fluorescence in most organic solvents but weak fluorescence in highly polar solvents, in particular, in aqueous media. Such environment-sensitive properties of dipolar dyes have been importantly exploited for the environment-sensitive fluorescent probes.[16] Interestingly, the new dyes exhibited more pronounced emission change to solvent polarity compared to acedan. For example, dye **1** emits strongly in dichloromethane and acetonitrile, weakly in ethanol, and poorly in PBS buffer, whereas acedan emits strongly in dichloromethane and acetonitrile, moderately in ethanol, and weakly in PBS buffer (Figure 2). Other derivatives **2**−**4** also

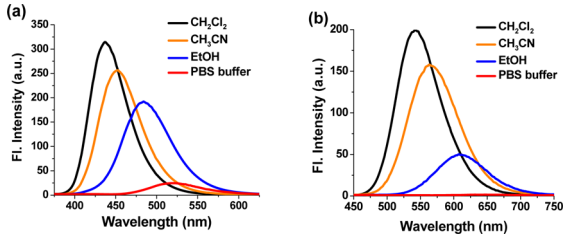


**Figure 2.** Fluorescence emission spectra of (a) acedan and (b) **1** in different solvents: dichloromethane, acetonitrile, ethanol, and PBS buffer (10 mM, pH 7.4, containing 0.1% DMSO). The fluorescence emission spectra were measured under excitation at the maximum absorption wavelength of each compound in the given solvent (10 $\mu$M) at 25 °C.

show similar emission behavior depending on the solvent polarity except **4** that shows very weak fluorescence in protic solvents, plausibly due to formation of the corresponding hydrate which has smaller ICT character (Supporting Information Figure S2).

The highly environment-sensitive nature of the new dyes is an added value for the development of environment-sensitive fluorescent probes. An important application of such environment-sensitive dyes can be found in fluorescence imaging of amyloid-$\beta$ plaques, a key pathological biomarker of Alzheimer's disease.[18]

To demonstrate important aspects of the new dyes in bioimaging, we carried out *ex vivo* two-photon fluorescence imaging of tissues stained with the representative dye **1**, and the results were compared with those stained with acedan. The tissue slice samples were prepared from several mouse organs (brain, liver, kidney, spleen, and lung) under usual fixative conditions, which were stained by incubating with **1** and acedan (each at 10 $\mu$M concentration), respectively, for 10 min and then washed with PBS buffer (for details, see Experimental Section). Samples of dye-untreated tissues were separately prepared as control for measuring the autofluorescence generated from the intrinsic fluorophores in tissues.

The TPM images shown in Figure 3 are not data-processed but intact images, which highlight the importance of excitation

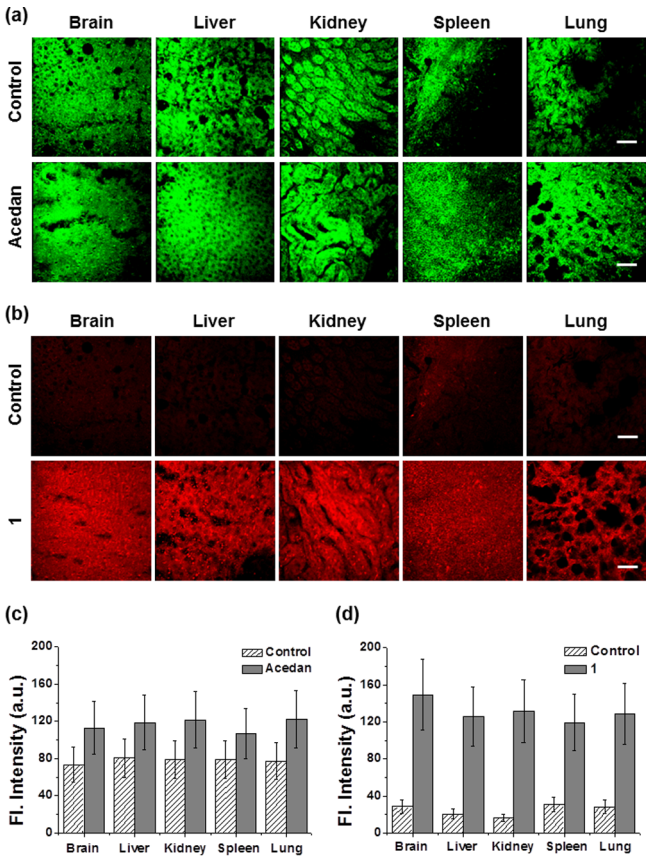


**Figure 3.** TPM images of tissues of different mouse organs, acquired with acedan and **1**, respectively, at a middle depth (~20 $\mu$m) of the sectioned tissues (thickness ~50 $\mu$m). (a) Images of tissues of brain, liver, kidney, spleen, and lung from the left, stained with acedan (10 $\mu$M) and at 37 °C for 10 min, observed under excitation at 780 nm. (b) The tissue images obtained under otherwise the same conditions except by staining with **1** and irradiating at 900 nm. Dye-untreated tissues were used as controls. Laser power was ~10 mW at the focal point in all cases. Scale bar is 50 $\mu$m. (c and d) Plots of the relative fluorescence intensity of the tissue images between the control and the dye-treated samples shown in (a) and (b), respectively.

at the longer wavelength at ~900 nm and emission in the red region (≥600 nm) to suppress the autofluorescence from the intrinsic fluorophores in tissues.

The TPM images of all of the different organs stained with acedan show strong autofluorescence when excited at 780 nm (Figure 3a), whereas those stained with $\pi$-extended acedan **1** show minimal autofluorescence when excited at 900 nm with


DOI: 10.1021/jacs.5b03548
J. Am. Chem. Soc. 2015, 137, 6781−6789

the same excitation laser power of ~10 mW at the focal point (Figure 3b). Typically, the laser power of ~10 mW or higher at the focal point is used to obtain bright tissue images under two-photon excitation conditions. When we applied a lower laser power of ~6 mW at the focal point, essentially the same trend was observed but with dim images (see Supporting Information Figure S10). The image data show that, in the case of acedan-incubated tissue images, there is slight differences in the intensity between the dye-treated and untreated ones when observed by naked eyes: Only the relative fluorescence intensity plots show small differences in the intensity, which, after data processing, are represented as the images in literature. Such processed data images may not properly represent the dye emission, because the control-subtracted intensity has a similar level of magnitude to that of the error bars. The relative fluorescence intensity plots of the respective images point out an important feature of such a $\pi$-extended dye system for tissue imaging, in addition to demonstrating that the significant autofluorescence results when a dye with shorter excitation/emission wavelengths is used (Figure 3c, 3d).

Comparison of the autofluorescence depending on the emission window, that is, below 560 nm (blue and green) versus above 560 nm (yellow and red), from the control tissues image data (dye-untreated) again shows that in both windows the excitation at 780 nm causes much higher autofluorescence than the exciation at 900 nm (Supporting Information Figure S11). As the red dye ($\pi$-extended acedan **1**) and the green dye (acedan) show comparable brightness in the different organ tissues (Supporting Information Figure S12), the tissue imaging data obtained with $\pi$-extended dye **1** thus show much lower autofluorescence than those obtained with acedan.

Autofluorescence from the intrinsic biomolecules under two-photon excitation conditions is well established. Efforts to suppress autofluorescence by different experimental setups have been made,[19] but the known methods are not straightforward. The autofluorescence is inevitable in most cases, and indeed it is used to investigate biological proceses including NAD/NADH redox process.[20] Disclosed here is that the strong autofluorescence observable by two-photon imaging at the shorter wavelength region of the biological optical window (780 nm) for tissue samples prepared under usual fixitive conditions can be greatly overcome by using a dye that can be excited and emit at the longer wavelength region ($\lambda_{ex}$ ~900 nm; $\lambda_{em}$ ≥600 nm). Then, what makes such a big difference? Although the two-photon absorption cross-section values of riboflavins and NADH, major contributors to the intrinsic autofluorescence, are much smaller (<1 GM) than those of dyes used here,[7] their biological concentrations are expected to be significantly higher than those of the dyes used here. If we count on the fact that dye's cell permeability/retention percentage is not complete, the relative concentrations of the intrinsic fluorophors with respect to those of dyes would be more than the value that can be estimated based on the probe concentration used. As a result, the intrinsic biomolecules seem to absorb and emit significant fluorescence, particularly when excited at the short NIR wavelength of 780 nm or so. It should be also noted that the intrinsic biomolecules except riboflavins exhibit decreasing two-photon absorbing behavior as the wavelength increases and reaches a minium around 900 nm (riboflavin shows a rather slow decrease).[7a] Surely, we should count on the reabsorption/emission process: acedan emits in the green region, which light can be best absorbed by riboflavins; in contrast, the dye **1** emits in the red region, a wavelength region where most of intrinsic fluorophores in tissues barely absorb. All these factors are conceivable for the contrasting imaging results observed here.

We have briefly checked whether dye **1** is localized in a specific organelle in cells by colocalization experiments using commercial reference dyes for lysosomes and mitochondria, respectively, that emit in the green region ($\lambda_{em}$ = 488 nm). The results show that dye **1** does not exhibit specific localization in these organelles and also in nuclei, but mostly distributes to cytosol (Supporting Information Figure S13).

The new dyes **1**–**4** have good solubility both in most organic solvents and in the aqueous buffer solution suitable for sensing purposes (Supporting Information Figure S5), in addition to having good cell-permeability; hence, use of them for the development of two-photon fluorescent probes or tags for analytes of biological interest is highly anticipated in the future.

***In Vivo* Two-Photon Imaging of Amyloid-$\beta$ Plaques.** One of important research areas of the environment-sensitive $\pi$-extended dipolar dyes can be found *in vivo* imaging of amyloid-$\beta$ (A$\beta$) plaques. A$\beta$ plaques have been considered as a key biomarker for Alzheimer's disease (AD), the most common neurodegenerative disease.[18] A$\beta$40 or A$\beta$42 monomers, which are produced from the amyloid precursor protein (APP) by secretase activities, aggregates to form amyloid plaques that exhibit a cross-$\beta$ sheet structure.[21] The cross-$\beta$ sheet structure provides a hydrophobic environment inside and a hydrophilic environment outside. Most of existing probes for imaging of A$\beta$ plaques are thus based on dyes that show environment-sensitive emission behavior.[22]

As our dipolar dyes show pronounced environment-sensitive emission behavior from that of acedan as well as little autofluorescence in tissue imaging, their application to *in vivo* imaging of A$\beta$ plaques is of great interest. To this end, we have synthesized compound **5** (Scheme 3), a cyclic analogue of the

**Scheme 3. Structure of A$\beta$ Probe 5 and Its Acyclic Analogue 6**

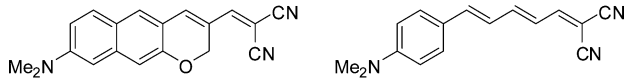


A$\beta$ probe **5** **6** (Ono *et al.*)

recently reported A$\beta$ probe **6** that allowed imaging of A$\beta$ plaques in near-infrared (NIR) wavelength region by OPM.[22d] Our probe **5** is expected to be photochemically more stable in general and also emit stronger fluorescence than the acyclic analogue **6**, as the former has less free-rotating bonds than the latter. Indeed, compound **5** allowed us to image A$\beta$ plaques under two-photon excitation conditions with negligible background signal as well as minimum photobleaching even after a long irradiation period at a much higher laser power.

The $\pi$-extended acedan **5** exhibited the longest maximum absorption and emission wavelengths among the new dipolar dyes, owing to the additional conjugation and enhanced ICT: $\lambda_{abs}$ = 512 nm, $\varepsilon$ = 16 700 L mol$^{-1}$ cm$^{-1}$, $\lambda_{em}$ = 679 nm, $\Phi_F$ = 5% in EtOH; $\Phi_F$ = 9% in $CH_3CN$ and 14% in $CH_2Cl_2$. (Supporting Information Figure S7). A desirable probe for imaging of A$\beta$ plaques should show strong fluorescence upon binding to A$\beta$ plaques, whereas it should emit negligiable fluorescence in the presence of serum albumin. Thus, we compared the fluorescence intensity of probe **5** in aqueous media in the presence or absence of A$\beta$42 aggregates and


DOI: 10.1021/jacs.5b03548
J. Am. Chem. Soc. 2015, 137, 6781–6789

bovine serum albumin (BSA), respectively, in pH 7.4 PBS buffer as well as in artificial cerebrospinal fluid (aCSF, see the composition in Experimental Section). Gratifyingly, probe **5** showed large fluorescence enhancement (41- to 60-fold) upon binding with A$\beta$42 aggregates and with negligible interference from BSA (Figure 4), in contrast to the acyclic analogue **6** and

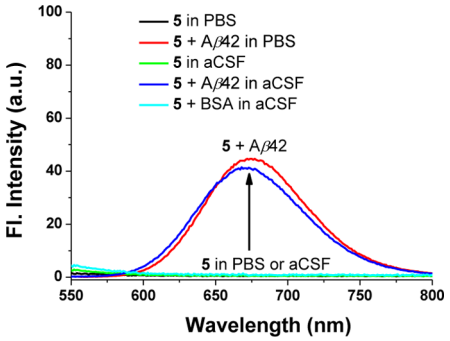


**Figure 4.** Fluorescence changes of probe **5** (10 $\mu$M) in the presence or absence of A$\beta$42 aggregates (20 $\mu$M) and BSA (20 $\mu$g mL$^{-1}$) in PBS buffer (10 mM, pH 7.4, containing 1% DMSO) or in artificial cerebrospinal fluid (aCSF, containing 1% DMSO), measured at 25 °C after mixing for 1 h under excitation at 500 nm.

other A$\beta$ imaging dyes that showed significant interference from BSA.[22d] The dissociation constant of compound **5** with A$\beta$42 aggregates was determined to be $K_d$ = 44.6 ± 4.2 nM (for details, see the Supporting Information), a comparable value to that observed with **6** ($K_d$ = 26.9 nM).

Given that probe **5** is biocompatible and responds to A$\beta$42 aggregates in the fluorescence turn-on type mode and, in particular, with negligible background signal, we have investigated its application to *in vivo* imaging of A$\beta$ plaques in a live AD mouse model. A prerequisite for *in vivo* imaging of A$\beta$ plagues is that the probe should pass the blood–brain barrier (BBB), which property is governed by several factors including the molecular size, charge density, and lipophilicity. The lipophilicity of compound **5** was calculated to be log $P$ = 3.5, which is close to the optimal value range considered for the BBB permeation (2.0–3.5).[22d] Thus, we expected that compound **5**, along with the favorable three factors mentioned, might penetrate the BBB.

Probe **5** was intraperitoneally injected into the 5XFAD mouse (10 mg kg$^{-1}$, one time injection). After 24 h, open-skull craniotomy surgery was performed (see Experimental Section) and fluorescence images of the brain were obtained under two-photon excitation at 1000 nm (Figure 5). Clear and bright red fluorescence images of A$\beta$ plaques were obtained owing to little autofluorescence outside the plaques, showing very promising features of the dye system for *in vivo* imaging. In addition, the *in vivo* imaging data confirms that probe **5** readily penetrates BBB. The 3D images obtained down to 300 $\mu$m depth show that A$\beta$ plaques are spreading out to the cortex region[23] (Figure 5c side view). Owing to our instrument's limitations, we were not able to look into the deeper region; however, it is clear that two-photon excitation at 1000 nm would allow deeper tissue imaging with proper instrumentation.[24] Specific A$\beta$ plaques of various sizes and in different shapes can be clearly visualized at different depths. Co-staining experiments with MeO-X04, a well-known A$\beta$ plaque staining fluorescent probe,[25] showed well-merged fluorescence images, confirming that probe **5** efficiently images A$\beta$ plaques (Figure 6). In addition,

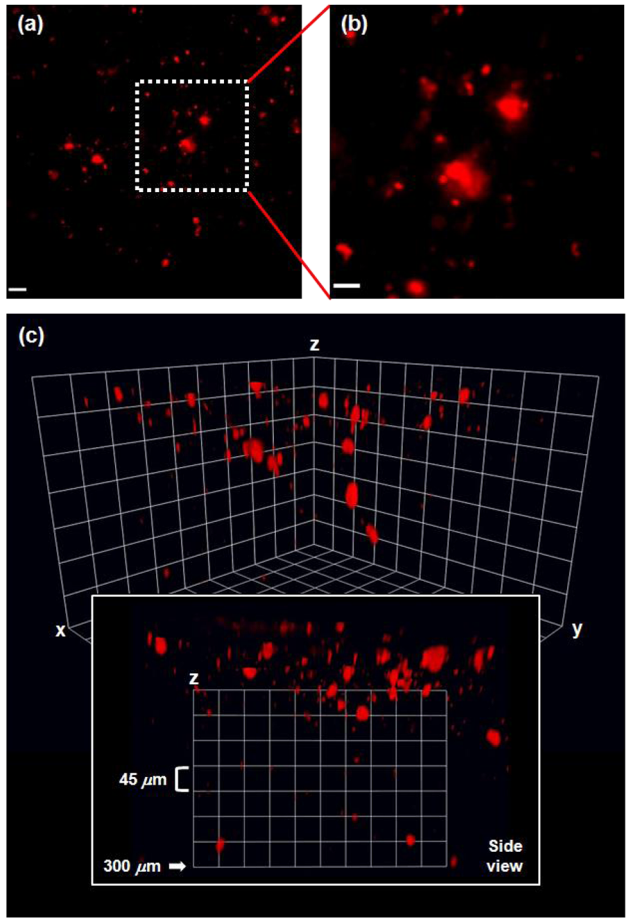


**Figure 5.** (a) *In vivo* TPM images of A$\beta$ plaques in the frontal cortex of a 5XFAD mouse after ip injection of **5** (10 mg kg$^{-1}$), 20× magnified at the depth of 50 $\mu$m (scale bar: 20 $\mu$m). (b) Magnified images (60×) of the square area in (a) (scale bar: 10 $\mu$m). (c) 3D images: the images were acquired with 20× magnification along the $z$-direction at the depth of up to 300 $\mu$m from the surface of the cortex, under excitation at 1000 nm with approximately 50 mW laser power at the focal point.

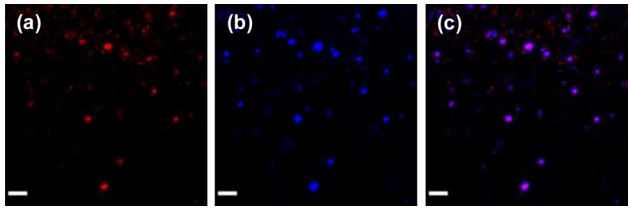


**Figure 6.** *In vivo* TPM images of A$\beta$ plaques in the frontal cortex of 5XFAD mouse costained with **5** and MeO-X04 (10 mg kg$^{-1}$ for each dye). The images were observed under excitation at (a) 1000 nm and (b) 780 nm, at the depth of 50 $\mu$m. (c) Merged image. Laser power was approximately 50 mW at the focal point. Scale bar is 30 $\mu$m.

reasonable photostability by two-photon laser irradiation in living stage and low cytotoxicity are additional assets of probe **5** (Supporting Information Figures S14 and S15).

## CONCLUSION

In summary, we have demonstrated that two-photon absorbing dyes that can be excited at the longer wavelength region of the first biological optical window greatly suppress autofluorescence in tissue imaging. Specifically, we have disclosed a new type of $\pi$-extended dyes, which provides negligible autofluor-


DOI: 10.1021/jacs.5b03548
J. Am. Chem. Soc. 2015, 137, 6781–6789

escence in tissue imaging under two-photon excitation at 900 nm wavelength. Considering they are readily accessible in few steps, have compact molecular sizes and good solubility in buffer media, the new dyes are highly promising for *in vivo* applications. Also sufficient two-photon absorption properties of two of the dyes appeal their use in bioimaging by two-photon microscopy. In addition, the new dyes showed more pronounced environment-sensitive emission behavior compared with acedan, a widely used two-photon absorbing dye in two-photon fluorescent probes, which property was exploited in the development of a novel two-photon imaging probe for A$\beta$ plaques. The new probe excitable at 1000 nm under two-photon excitation conditions was photochemically stable, biocompatible, and readily penetrated the blood−brain barrier, allowing *in vivo* fluorescence imaging of A$\beta$ plaques in a live mouse model of Alzheimer's disease. The results show clear fluorescence images of the plaques spreading out to the cortex region, with negligible background signal. The new dye system is thus highly promising for the development of two-photon probes for bioimaging purposes, which is under active investigation. Also, the two-photon probe for A$\beta$ plaques offers us a valuable tool for *in vivo* monitoring of A$\beta$ plaques in Alzheimer's disease animal models.

## EXPERIMENTAL SECTION

**General Information.** The chemical reagents were purchased from Aldrich or TCI. Commercially available reagents were used without further purification. Anhydrous solvents for organic synthesis were prepared by passing through a solvent purification tower. All reactions were performed under argon atmosphere unless otherwise stated. Thin-layer chromatography (TLC) was performed on pre-coated silica gel 60F-254 glass plates. $^1$H and $^{13}$C NMR spectra were measured with a Bruker AVANCE III 300 MHz and AVANCE III 600 MHz FT-NMR spectrometer. Coupling constants ($J$ value) are reported in hertz. The chemical shifts ($\delta$) are shown in ppm, multiplicities are indicated by s (singlet), d (doublet), t (triplet), dd (doublet of doublets), and m (multiplet). Spectra are referenced to residual chloroform (7.26 ppm, $^1$H, 77.16 ppm, $^{13}$C). UV/vis absorption spectra were obtained using a HP 8453 UV/vis spectrophotometer. Fluorescence emission spectra were recorded on a Photon Technical International Fluorescence System with a 1 cm standard quartz cell. High-resolution mass spectra was recorded on a JEOL JMS-700 spectrometer at the Korea Basic Science Center, Kyungpook National University and the values are reported in units of mass to charge ($m/z$). Log $P$ values were calculated using ACDLab-ACDLogP program, which is available at http://www.acdlabs.com/resources/freeware.

**Synthesis.** *6-(Dimethylamino)-3-hydroxy-2-naphthaldehyde (**7**).* Compound **7** was synthesized according to the procedures previously reported by us.[10]

*8-(Dimethylamino)-2,3,4,4a-tetrahydro-1H-benzo[b]xanthen-1-one (**1**).* A solution of compound **7** (110 mg, 0.50 mmol), 2-cyclohexen-1-one (97 $\mu$L, 1.0 mmol), and 1,4-diazabicyclo[2.2.2]-octane (DABCO, 28 mg, 0.25 mmol) in $H_2O$/1,4-dioxane (3.0 mL, 1:2, v/v) was taken in a capped vial and stirred at 45−50 °C under sonication for 48 h. The solvent was evaporated under reduced pressure to give the crude product as dark red residue. The residue was purified by flash silica gel column chromatography (eluent: EtOAc/hexane = 1/9) to give compound **1** as a orange solid (56 mg, 38%; 40% of compound **7** was recovered). $^1$H NMR ($CDCl_3$, 300 MHz, 297 K): $\delta$ 7.61−7.54 (m, 3H), 6.99−6.95 (m, 2H), 6.69 (d, $J$ = 2.1 Hz, 1H), 5.04−4.97 (m, 1H), 3.07 (s, 6H), 2.64−2.35 (m, 3H), 2.14−1.95 (m, 2H), 1.81−1.66 (m, 1H). $^{13}$C NMR ($CDCl_3$, 75 MHz, 298 K): $\delta$ 197.4, 153.2, 149.9, 137.9, 132.1, 130.7, 130.3, 129.6, 122.7, 119.2, 114.4, 109.1, 104.8, 74.8, 40.5 (2 carbons), 38.8, 29.9, 18.1. HRMS: $m/z$ calcd for $C_{19}H_{19}NO_2$, 293.3597; found, 293.1417.

*7-(Dimethylamino)-3,3a-dihydrobenzo[g]cyclopenta[b]-chromen-1(2H)-one (**2**).* A solution of compound **7** (20 mg, 0.094 mmol), 2-cyclohexen-1-one (48 $\mu$L, 0.56 mmol), and 1,4-diazabicyclo[2.2.2]octane (DABCO, 11 mg, 0.095 mmol) in $H_2O$/1,4-dioxane (1.8 mL, 1:1, v/v) was taken in a capped vial and stirred at 45−50 °C under sonication for 48 h. The reaction mixture was partitioned between EtOAc and $H_2O$, and then the organic layer was separated. The aqueous layer was further extracted twice with EtOAc, and the combined organic extracts were washed with brine, dried over anhydrous $Na_2SO_4$. The solvent evaporated under reduced pressure, and the crude product was purified by flash silica gel column chromatography (eluent: EtOAc/hexane = 5/95 to 1/9) to give compound **2** as a yellow solid (5.7 mg, 22%; 70% of compound **7** was recovered). $^1$H NMR ($CDCl_3$, 300 MHz, 296 K): $\delta$ 7.60 (d, $J$ = 9.0 Hz, 1H), 7.57 (s, 1H), 7.37 (d, $J$ = 2.1 Hz, 1H), 7.02 (s, 1H), 6.98 (dd, $J$ = 9.0 2.4 Hz, 1H), 6.69 (d, $J$ = 2.4 Hz, 1H), 5.31−5.25 (m, 1H), 3.08 (s, 6H), 2.76−2.56 (m, 2H), 2.44−2.31 (m, 1H), 2.22−2.11 (m, 1H);. $^{13}$C NMR ($CDCl_3$, 75 MHz, 297 K): $\delta$ 201.4, 152.8, 150.0, 138.0, 132.0, 131.2, 129.6, 128.5, 122.7, 118.8, 114.5, 109.8, 104.8, 76.1, 40.5 (2 carbons), 37.1, 28.2. HRMS: $m/z$ calcd for $C_{18}H_{17}NO_2$, 279.3331; found, 279.1260.

*1-(8-(Dimethylamino)-2H-benzo[g]chromen-3-yl)ethanone (**3**).* To a solution of compound **7** (200 mg, 0.70 mmol) and 3-buten-2-one (170 $\mu$L, 2.1 mmol) in MeOH (5.0 mL) at 25 °C under argon was added a solution of $MgI_2$ (20 mg, 0.070 mmol) and tetramethylethylenediamine (TMEDA, 11 $\mu$L, 0.070 mmol) in MeOH (1.0 mL), followed by dropwise addition of a solution of 4-dimethylaminopyridine (DMAP, 8.6 mg, 0.070 mmol) in MeOH (0.50 mL). The resulting mixture was stirred at 25 °C under argon for 24 h, and then the reaction was quenched by addition of saturated aqueous $NH_4Cl$ solution (2.0 mL). The reaction mixture was extracted with dichloromethane (2 × 20 mL) and dried over anhydrous $Na_2SO_4$. The solvent evaporated under reduced pressure, and the crude product was purified by flash silica gel column chromatography (eluent: EtOAc/hexane = 1/9) to give compound **3** as a yellow solid (70 mg, 28%; 37% of compound **7** was recovered). $^1$H NMR ($CDCl_3$, 300 MHz, 297 K): $\delta$ 7.59 (d, $J$ = 9.0 Hz, 1H), 7.48 (s, 1H), 7.44 (s, 1H), 6.98−6.94 (m, 2H), 6.69 (d, $J$ = 2.4 Hz, 1H), 5.02 (d, $J$ = 1.2 Hz, 2H), 3.07, (s, 6H), 2.42 (s, 3H). $^{13}$C NMR ($CDCl_3$, 75 MHz, 298 K): $\delta$ 195.9, 152.8, 149.9, 138.2, 134.6, 131.0, 129.5, 129.5, 122.5, 117.9, 114.3, 109.3, 104.8, 64.5, 40.5 (2 carbons), 25.0. HRMS: $m/z$ calcd for $C_{17}H_{17}NO_2$, 267.3224; found, 267.1257.

*6-(Dimethylamino)-3-(prop-2-ynyloxy)-2-naphthaldehyde (**8**).* To a solution of compound **7** (200 mg, 0.93 mmol) and $K_2CO_3$ (390 mg, 2.8 mmol) in DMF (6.5 mL) at 25 °C was added propargyl bromide (80 wt % solution in $PhCH_3$, 0.20 mL, 1.4 mmol). The resulting mixture was stirred at 25 °C for 12 h. The reaction mixture was partitioned between EtOAc and $H_2O$, and then the organic layer was separated. The aqueous layer was further extracted twice with EtOAc, and the combined organic extracts were washed with brine, dried over anhydrous $Na_2SO_4$, and concentrated to give a crude product **7**, which was used for the next step without further purification.

*8-(Dimethylamino)-2H-benzo[g]chromene-3-carbaldehyde (**4**).*[12] A solution of compound **8** (37 mg, 0.15 mmol) and CuI (57 mg, 0.30 mmol) in $CH_3CN$ (3.7 mL) was stirred at 82 °C for 48 h. The solvent was evaporated under reduced pressure, and the crude product was purified by flash silica gel column chromatography (eluent: EtOAc/hexane = 5/95) to give compound **4** as a orange solid (70 mg, 71%). $^1$H NMR ($CDCl_3$, 300 MHz, 298 K): $\delta$ 10.39 (s, 1H), 8.11 (s, 1H), 7.69 (d, $J$ = 9.3 Hz, 1H), 7.05−6.98 (m, 2H), 6.78 (d, $J$ = 2.1 Hz, 1H), 5.96−5.90 (m, 1H), 4.91 (dd, $J$ = 3.9, 1.8 Hz, 2H), 3.13 (s, 6H). $^{13}$C NMR ($CDCl_3$, 75 MHz, 298 K): $\delta$ 189.5, 153.6, 150.8, 135.1, 132.1, 130.2, 121.2, 121.1, 120.6, 119.3, 114.3, 113.8, 98.9, 65.2, 40.4 (2 carbons). HRMS: $m/z$ calcd for $C_{16}H_{15}NO_2$, 253.2958; found, 253.1100.

*2-{[(8-Dimethylamino)-2H-benzo[g]chromen-3-yl]methylene}-malononitrile (**5**).* To a solution of compound **4** (220 mg, 0.93 mmol), malononitrile (62 mg, 0.93 mmol), and CuI (53 mg, 0.28 mmol) in $CH_3CN$ (6.0 mL) was added $Et_3N$ (0.10 mL, 0.090 mmol).


DOI: 10.1021/jacs.5b03548
J. Am. Chem. Soc. 2015, 137, 6781−6789

The resulting mixture was stirred at 75 °C for 4 h. The solvent was evaporated under reduced pressure, and the crude product was purified by flash silica gel column chromatography (eluent: dichloromethane) to give compound **5** as a red solid (200 mg, 70%). $^1$H NMR ($CDCl_3$, 600 MHz, 293 K): $\delta$ 7.61 (d, $J$ = 9.0 Hz, 1H), 7.51 (s, 1H), 7.27 (s, 1H), 7.23 (s, 1H), 6.99 (dd, $J$ = 9.3, 2.7 Hz, 1H), 6.97 (s, 1H), 6.69 (d, $J$ = 2.4 Hz, 1H), 5.39 (s, 2H), 3.14 (s, 6H). $^{13}$C NMR ($CDCl_3$, 150 MHz, 293 K): $\delta$ 155.5, 152.4, 150.7, 142.5, 139.5, 131.4, 130.4, 126.8, 122.7, 117.9, 114.9, 114.5, 113.7, 109.3, 104.5, 64.5, 40.3 (2 carbons). HRMS: $m/z$ calcd for $C_{19}H_{15}ON_3$, 301.1215; found, 301.1215.

***In Vitro* Assay of $\pi$-Extended Acedan Derivative 5.** Amyloid-$\beta$ (A$\beta$) plaques were prepared as known procedure.[26] Briefly, A$\beta$42 (Sigma-Aldrich, A9810, MW = 4514.04, 1 mg) was dissolved in PBS buffer (10 mM, pH 7.4) to a final concentration of 100 $\mu$M. This solution was incubated in e-tube shaker (60 rpm, F1 mode of SLRM-2M, MyLab Corp.) at 25 °C for 3 days, and used for *in vitro* assay directly. Incubation of aggregated A$\beta$ with compound **5** was carried out with the same incubating condition for 1 h. Bovine serum albumin (BSA, Promega, R396D) was prepared using a 10 mg mL$^{-1}$ stock solution in PBS buffer (10 mM, pH 7.4). The composition of artificial cerebrospinal fluid (aCSF) was NaCl (124 mM), KCl (3 mM), $NaH_2PO_4$ (1.25 mM), $MgCl_2$ (1 mM), $NaHCO_3$ (36 mM), D-glucose (10 mM), $CaCl_2$ (2 mM), 95% $O_2$, and 5% $CO_2$ (by bubbler).

**Preparation of the *ex Vivo* Mouse Tissue Samples.** C57BL6 type mouse (5 weeks, male, SAMTAKO Corp.) was used for this experiment. Basically, experiment was done on light protected conditions: dark-room and aluminum foil. The mouse was dissected to five organs: brain, liver, kidney, spleen, and lung. These organs were washed several times with phosphate buffered saline (PBS) buffer. After washes, each organ was frozen using dry ice for 5 min. After that, frozen organs were crushed with a hammer. Tissue slice samples were made by section machine (Cryostat machine, Leica, CM3000 model) at 50 $\mu$m thicknesses. For organ fixation on this section machine, we used OCT compound (optimal cutting temperature compound: 10% w/w poly(vinyl alcohol), 25% w/w polyethylene glycol, and 85.5% w/w inactive species). Tissue slice samples were placed on the specimen block (Paul Marienfeld GmbH & Co.). These specimen blocks were immersed on 4% paraformaldehyde for 10 min. After tissue fixation, specimen blocks were washed several times with PBS buffer. After washes, tissues were fixed again using mount solution (Gel Mount, BIOMEDA). After preparation of the staining solution of acedan (10 $\mu$M in PBS buffer containing 1% DMSO) and **1** (10 $\mu$M in PBS buffer containing 1% DMSO), the prepared tissue sample slides were dipped into the staining solution at 37 °C for 10 min, then washed three times with PBS and mounted. Two-photon microscopy (TPM) imaging experiments were done after mount solution became hard.

***Ex Vivo* Two-Photon Microscopy Imaging of Mouse Tissues Stained with Dyes.** We used TPM based on a developed upright microscope (BX51, Olympus) for advanced performance of deep tissue imaging. TPM had 20× objective lens (XLUMPlanFLN, Olympus) with 1.0 numerical aperture (NA). The objective lens focused the excitation beam into tissue samples. The excitation focus scanned in the $x-y$ plane of the sample by the resonant scanner (GSI Lumonics, 8 kHz resonant frequency) and galvanometric scanner (6215H, Cambridge Technology), and in the $z$-axis by an objective translator (P-725.4CL, PI) through the two dichroic mirrors (1025DCSP, 680DCSP, Hamamatsu). The emission light from the sample was collected back by the objective lens and was reflected on dichroic mirror (680DCLP, Chroma) toward photomultiplier tubes (PMTs, H7421-40, Hamamatsu). Signals from the PMTs were collected by a frame grabber (Alta, Bitflow) and images were displayed in real time. Data were processed using Matlab and Amira tools. The excitation laser was tuned to 780 and 900 nm for acedan and compound **1** fluorescence signals, respectively. Power of the excitation laser was approximately 10 mW at the focal point. The imaging field-of-view was 250 $\mu$m × 250 $\mu$m consisting of 512 × 512 pixels, and the imaging speed was 0.1 frames s$^{-1}$.

**Animals.** Thirteen month-old Alzheimer's disease animal model mice, 5XFAD mice (The Jackson Laboratory, Bar Harbor, ME; stock no. 006554, Tg6799), were used for two-photon *in vivo* imaging. The mice have Swedish, Florida, and London human APP 695 mutation and M146L and L286 V human presenilin-1 mutation.[27] Therefore, A$\beta$ plaques, one of the major pathological hallmarks of AD, are aggressively expressed from 3 months of age. In 13 months, the age which we used, massive A$\beta$ plaque loads exist in the brain of 5XFAD mice and the phenotypes of AD are clearly shown. All animal treatments and experiments were performed and approved by the Ethics Review Committee for Animal Experimentation in Seoul National University.

**Craniotomy Surgery.** Open-skull craniotomy surgery was performed to visualize A$\beta$ plaques *in vivo* with compound **5** and MeO-X04, as described.[26,28] Shortly, Zoletil 50 (Virbac; intramuscular injection, 0.03 mL) was used to anesthetize and the mouse was fixed on the customized stereotactic heating plate (Live Cell Instruments, Seoul, Korea; 37 °C). After removing the scalp and the periosteum, the region (1 mm from bregma, 1 mm from sagittal suture; diameter, 3 mm) of the skull was drilled with a microdrill. Then, the bone was removed laboriously. A 3 mm-round coverslip was attached to the region with Loctite 454. Lastly, emerged portions of the skull were covered with dental acryl. The anti-inflammatory drug mixture (dexamethasone (0.2 mg kg$^{-1}$) and carprofen (5 mg kg$^{-1}$)) was treated just before and after the surgery, respectively.

***In Vivo* Two-Photon Microscopic Imaging of Alzheimer's Disease Mouse Brain.** The two-photon confocal microscope was purchased from Carl Zeiss Microscopy GmbH (Oberkochen, Germany; model no. LSM 7 MP two-photon laser scanning microscope system). To visualize A$\beta$ plaques, compound **5** (10 mg kg$^{-1}$; 10% of the stock (30 mg mL$^{-1}$ in DMSO), 45% of propylene glycol, 45% of PBS) or MeO-X04 (10 mg kg$^{-1}$; 10% of the stock (50 mg mL$^{-1}$ in DMSO), 45% of propylene glycol, 45% of PBS) was intraperitoneally injected into a mouse 24 h before imaging.[29] For the imaging of MeO-X04 and **5**, excitation wavelengths at 780 nm and at 1000 nm were used, respectively. To obtain the 3D images, z-stack imaging was performed at intervals of 1 $\mu$m and up to 300 $\mu$m. Image processing was carried out by Volocity software (PerkinElmer, Inc., MA).

**Cell Viability Assay.** Cell viability was assessed by measuring ability of a compound to metabolize 3-(4,5-dimethyldiazol-2-yl)-2,5-diphenyltetrazolium bromide (MTT) to formazan in SHSY5Y cell line.[30] Cells (100 $\mu$L well$^{-1}$) were seeded at a density of about 5 × 10$^3$ cells per well into 96-well plates and incubated until 70−80% confluency. The cells were treated with 1, 5, 10, 20, and 50 $\mu$M of compounds **1** and **5**, respectively, and incubated for 1 h, and then the cells were washed with PBS buffer. Twenty-five microliters of MTT solution (5 mg mL$^{-1}$) was added to each well, and cells were maintained for 2 h at 37 °C. Media was removed and the formazan crystals trapped in cells were dissolved in sterile DMSO (100 $\mu$L) by incubating at 37 °C for 2 h. The absorbance at 570 nm was measured in a plate reader.

## ■ ASSOCIATED CONTENT

### Ⓢ Supporting Information

Scheme, supporting figures, NMR and HR-Mass spectra. The Supporting Information is available free of charge on the ACS Publications website at DOI: 10.1021/jacs.5b03548.

## ■ AUTHOR INFORMATION


### Corresponding Author

*ahn@postech.ac.kr

### Author Contributions

‖These authors contributed equally.


### Notes

The authors declare the following competing financial interest(s): The authors are listed as inventors on a pending patent application related to technology described in this work.



DOI: 10.1021/jacs.5b03548
J. Am. Chem. Soc. 2015, 137, 6781−6789

## ■ ACKNOWLEDGMENTS

This work was supported by Ministry of Health & Welfare (HI13C1378) and by EPB Center (R11-2008-052-01001) and Global Research Laboratory Program (2014K1A1A2064569) through the National Research Foundation (NRF) funded by Ministry of Science, ICT & Future Planning. Prof. I. Mook-Jung thanks the financial support from NRF (2012R1A2A1A01002881, MRC [2011e0030738]) and Korea Institute of Science and Technology Institutional Program (2E24242-13e135). Prof. J. Jung thanks the financial support from NRF funded by Ministry of Education and Science Technology (No. 2011-0030072). Prof. K. H. Kim thanks the financial support from NRF (2014R1A2A1A12067510) funded by the Korea government (MEST). We thank Mr. Youngseob Jung in POSTECH for assessing cell viability and Dr. Chang Su Lim in Korea University for measuring the two-photon action spectra.

## ■ REFERENCES

(1) (a) Terai, T.; Nagano, T. *Curr. Opin. Chem. Biol.* **2008**, *12*, 515. (b) Kikuchi, K. *Chem. Soc. Rev.* **2010**, *39*, 2048. (c) Chan, J.; Dodani, S. C.; Chang, C. J. *Nat. Chem.* **2012**, *4*, 973. (d) Yang, Y.; Zhao, Q.; Feng, W.; Li, F. *Chem. Rev.* **2013**, *113*, 192.

(2) (a) Xu, C.; Zipfel, W.; Shear, J. B.; Williams, R. M.; Webb, W. W. *Proc. Natl. Acad. Sci. U.S.A.* **1996**, *93*, 10763. (b) Weissleder, R. *Nat. Biotechnol.* **2001**, *19*, 316. (c) Williams, R. M.; Zipfel, W. R.; Webb, W. W. *Curr. Opin. Chem. Biol.* **2001**, *5*, 603. (d) Zipfel, W. R.; Williams, R. M.; Webb, W. W. *Nat. Biotechnol.* **2003**, *21*, 1369. (e) Frangioni, J. V. *Curr. Opin. Chem. Biol.* **2003**, *7*, 626. (f) Helmchen, F.; Denk, W. *Nat. Methods.* **2005**, *2*, 932. (g) Rubart, M. *Circ. Res.* **2004**, *95*, 1154. (h) Pawlicki, M.; Collins, H. A.; Denning, R. G.; Anderson, H. L. *Angew. Chem., Int. Ed.* **2009**, *48*, 3244. (i) Hoover, E. E.; Squier, J. A. *Nat. Photonics* **2013**, *7*, 93.

(3) (a) Dombeck, D. A.; Khabbaz, A. N.; Collman, F.; Adelman, T. L.; Tank, D. W. *Neuron* **2007**, *56*, 43. (b) Fisher, J. A.; Barchi, J. R.; Welle, C. G.; Kim, G. H.; Kosterin, P.; Obaid, A. L.; Yodh, A. G.; Contreras, D.; Salzberg, B. M. *J. Neurophysiol.* **2008**, *99*, 1545. (c) Kim, H. M.; Seo, M. S.; An, M. J.; Hong, J. H.; Tian, Y. S.; Choi, J. H.; Kwon, O.; Lee, K. J.; Cho, B. R. *Angew. Chem., Int. Ed.* **2008**, *47*, 5167. (d) Kim, M. K.; Lim, C. S.; Hong, J. T.; Han, J. H.; Jang, H. Y.; Kim, H. M.; Cho, B. R. *Angew. Chem., Int. Ed.* **2010**, *49*, 364. (e) Lee, J. H.; Lim, C. S.; Tian, Y. S.; Han, J. H.; Cho, B. R. *J. Am. Chem. Soc.* **2010**, *132*, 1216. (f) Lim, C. S.; Masanta, G.; Kim, H. J.; Han, J. H.; Kim, H. M.; Cho, B. R. *J. Am. Chem. Soc.* **2011**, *133*, 11132. (g) Kim, D.; Singha, S.; Wang, T.; Seo, E.; Lee, J. H.; Lee, S. J.; Kim, K. H.; Ahn, K. H. *Chem. Commun.* **2012**, *48*, 10243. (h) Li, L.; Shen, X.; Xu, Q.-H.; Yao, S. Q. *Angew. Chem., Int. Ed.* **2013**, *52*, 424.

(4) (a) Kim, H. M.; Cho, B. R. *Chem. Asian J.* **2011**, *6*, 58. (b) Rao, A. S.; Kim, D.; Nam, H.; Jo, H.; Kim, K. H.; Ban, C.; Ahn, K. H. *Chem. Commun.* **2012**, *48*, 3206. (c) Kim, D.; Ryu, H. G.; Ahn, K. H. *Org. Biomol. Chem.* **2014**, *12*, 4550.

(5) (a) Kim, H. M.; An, M. J.; Hong, J. H.; Jeong, B. H.; Kwon, O.; Hyon, J. Y.; Hong, S. C.; Lee, K. J.; Cho, B. R. *Angew. Chem., Int. Ed.* **2008**, *47*, 2231. (b) Kim, H. M.; Cho, B. R. *Acc. Chem. Res.* **2009**, *42*, 863. (c) Li, L.; Zhang, C.-W.; Chen, G. Y. J.; Zhu, B.; Chai, C.; Xu, Q.-H.; Tan, E.-K.; Zhu, Q.; Lim, K.-L.; Yao, S. Q. *Nat. Commun.* **2014**, *5*, 3276.

(6) Rao, A. S.; Kim, D.; Wang, T.; Kim, K. H.; Hwang, S.; Ahn, K. H. *Org. Lett.* **2012**, *14*, 2598.

(7) (a) Zipfel, W. R.; Williams, R. M.; Christie, R.; Nikitin, A. Y.; Hyman, B. T.; Webb, W. W. *Proc. Natl. Acad. Sci. U.S.A.* **2003**, *100*, 7075. (b) Huang, S.; Heikal, A. A.; Webb, W. W. *Biophys. J.* **2002**, *82*, 2811. (c) Radosevich, A. J.; Bouchard, M. B.; Burgess, S. A.; Chen, B. R.; Hillman, E. M. C. *Opt. Lett.* **2008**, *33*, 2164. (d) Heo, C. H.; Kim, K. H.; Kim, H. J.; Baik, S. H.; Song, H.; Kim, Y. S.; Lee, J.; Mook-Jung, I.; Kim, H. M. *Chem. Commun.* **2013**, *49*, 1303.

(8) (a) Kobat, D.; Durst, M. E.; Nishimura, N.; Wong, A. W.; Schaffer, C. B.; Xu, C. *Opt. Express* **2009**, *17*, 13354. (b) Kobat, D.; Horton, N. G.; Xu, C. *J. Biomed. Opt.* **2011**, *16*, 106014.

(9) (a) Kim, H. M.; Jeong, B. H.; Hyon, J. Y.; An, M. J.; Seo, M. S.; Hong, J. H.; Lee, K. J.; Kim, C. H.; Joo, T.; Hong, S. C.; Cho, B. R. *J. Am. Chem. Soc.* **2008**, *130*, 4246. (b) Lim, C. S.; Kim, H. J.; Lee, J. H.; Tian, Y. S.; Kim, C. H.; Kim, H. M.; Joo, T.; Cho, B. R. *ChemBioChem* **2011**, *12*, 392.

(10) Kim, I.; Kim, D.; Sambasivan, S.; Ahn, K. H. *Asian J. Org. Chem.* **2012**, *1*, 60.

(11) Yuan, L.; Lin, W.; Chen, H.; Zhu, S.; He, L. *Angew. Chem., Int. Ed.* **2013**, *52*, 10018.

(12) Kumari, K.; Raghuvanshi, D. S.; Singh, K. N. *Tetrahedron* **2013**, *69*, 82.

(13) (a) Smith, A. M.; Mancini, M. C.; Nie, S. *Nat. Nanotechnol.* **2009**, *4*, 710. (b) Gao, X.; Cui, Y.; Levenson, R. M.; Chung, L. W.; Nie, S. *Nat. Biotechnol.* **2004**, *22*, 969. (c) Hilderbrand, S. A.; Weissleder, R. *Curr. Opin. Chem. Biol.* **2010**, *14*, 71.

(14) (a) Kim, H. M.; Kim, B. R.; Hong, J. H.; Park, J. S.; Lee, K. J.; Cho, B. R. *Angew. Chem., Int. Ed.* **2007**, *46*, 7445. (b) Kim, H. M.; Seo, M. S.; An, M. J.; Hong, J. H.; Tian, Y. S.; Choi, J. H.; Kwon, O.; Lee, K. J.; Cho, B. R. *Angew. Chem., Int. Ed.* **2008**, *47*, 5167.

(15) (a) Grabowski, Z. R.; Rotkiewicz, K.; Rettig, W. *Chem. Rev.* **2003**, *103*, 3899. (b) Fleisher, A. J.; Bird, R. G.; Zaleski, D. P.; Pate, B. H.; Pratt, D. W. *J. Phys. Chem. B* **2013**, *117*, 4231.

(16) (a) Jacobson, A.; Petric, A.; Hogenkamp, D.; Sinur, A.; Barrio, J. R. *J. Am. Chem. Soc.* **1996**, *118*, 5572. (b) Gaus, K.; Gratton, E.; Kable, E. P.; Jones, A. S.; Gelissen, I.; Kritharides, L.; Jessup, W. *Proc. Natl. Acad. Sci. U.S.A.* **2003**, *100*, 15554. (c) Kim, H. M.; Jung, C.; Kim, B. R.; Jung, S. Y.; Hong, J. H.; Ko, Y. G.; Lee, K. J.; Cho, B. R. *Angew. Chem., Int. Ed.* **2007**, *46*, 3460. (d) Kim, H. M.; Choo, H. J.; Jung, S. Y.; Ko, Y. G.; Park, W. H.; Jeon, S. J.; Kim, C. H.; Joo, T.; Cho, B. R. *ChemBioChem* **2007**, *8*, 553.

(17) Kim, D.; Sambasivan, S.; Nam, H.; Kim, K. H.; Kim, J. Y.; Joo, T.; Lee, K. H.; Kim, K. T.; Ahn, K. H. *Chem. Commun.* **2012**, *48*, 6833.

(18) (a) Mattson, M. P. *Nature* **2004**, *430*, 631. (b) Goedert, M.; Spillantini, M. G. *Science* **2006**, *314*, 777. (c) Kepp, K. P. *Chem. Rev.* **2012**, *112*, 5193. (d) Potter, H.; Dressler, D. *Nat. Biotechnol.* **2000**, *18*, 125.

(19) (a) Mansfield, J. R.; Gossage, K. W.; Hoyt, C. C.; Levenson, R. M. *J. Biomed. Optics* **2005**, *10*, 041207. (b) Steinkamp, J. A.; Stewart, C. C. *Cytometry* **1986**, *A7*, 566. (c) Viegas, M. S.; Martins, T. C.; Seco, F.; de Carmo, A. *Eur. J. Histochem.* **2007**, *51*, 59.

(20) (a) Aubin, J. E. *J. Histochem. Cytochem.* **1979**, *27*, 36. (b) Benson, R. C.; Meyer, R. A.; Zaruba, M. E.; McKhann, G. M. *J. Histochem. Cytochem.* **1979**, *27*, 44. (c) Yu, Q.; Heikal, A. A. *J. Photochem. Photobiol., B* **2009**, *95*, 46. (d) Skala, M. C.; Riching, K. M.; Gendron-Fitzpatrick, A.; Eickhoff, J.; Eliceiri, K. W.; White, J. G.; Ramanujam, N. *Proc. Natl. Acad. Sci. U.S.A.* **2007**, *104*, 19494.

(21) (a) Greenwald, J.; Riek, R. *Structure* **2010**, *18*, 1244. (b) Walsh, D. M.; Hartley, D. M.; Kusumoto, Y.; Fezoui, Y.; Condron, M. M.; Lomakin, A.; Benedek, G. B.; Selkoe, D. J.; Teplow, D. B. *J. Biol. Chem.* **1999**, *274*, 25945.

(22) (a) Hintersteiner, M.; Enz, A.; Frey, P.; Jaton, A. L.; Kinzy, W.; Kneuer, R.; Neumann, U.; Rudin, M.; Staufenbiel, M.; Stoeckli, M.; Wiederhold, K. H.; Gremlich, H. U. *Nat. Biotechnol.* **2005**, *23*, 577. (b) Ran, C.; Xu, X.; Raymond, S. B.; Ferrara, B. J.; Neal, K.; Bacskai, B. J.; Medarova, Z.; Moore, A. *J. Am. Chem. Soc.* **2009**, *131*, 15257. (c) Petric, A.; Johnson, S. A.; Pham, H. V.; Li, Y.; Ceh, S.; Golobic, A.; Agdeppa, E. D.; Timbol, G.; Liu, J.; Keum, G.; Satyamurthy, N.; Kepe, V.; Houk, K. N.; Barrio, J. R. *Proc. Natl. Acad. Sci. U.S.A.* **2012**, *109*, 16492. (d) Cui, M.; Ono, M.; Watanabe, H.; Kimura, H.; Liu, B.; Saji, H. *J. Am. Chem. Soc.* **2014**, *136*, 3388.

(23) Maezawa, I.; Hong, H. S.; Liu, R.; Wu, C. Y.; Cheng, R. H.; Kung, M. P.; Kung, H. F.; Lam, K. S.; Oddo, S.; Laferla, F. M.; Jin, L. W. *J. Neurochem.* **2008**, *104*, 457.

(24) In the commercial *Carl Zeiss* two-photon microscopy (see Supporting Information), the two-photon excitation laser power is



DOI: 10.1021/jacs.5b03548
*J. Am. Chem. Soc.* 2015, 137, 6781−6789

limited to use below 50 mW when two-photon excitation wavelength is 1000 nm or beyond it.
(25) Klunk, W. E.; Bacskai, B. J.; Mathis, C. A.; Kajdasz, S. T.; McLellan, M. E.; Frosch, M. P.; Debnath, M. L.; Holt, D. P.; Wang, Y. M.; Hyman, B. T. *J. Neuropathol. Exp. Neurol.* **2002**, *61*, 797.
(26) Baik, S. H.; Cha, M. Y.; Hyun, Y. M.; Cho, H.; Hamza, B.; Kim, D. K.; Han, S. H.; Choi, H.; Kim, K. H.; Moon, M.; Lee, J.; Kim, M.; Irimia, D.; Mook-Jung, I. *Neurobiol. Aging* **2014**, *35*, 1286.
(27) Oakley, H.; Cole, S. L.; Logan, S.; Maus, E.; Shao, P.; Craft, J.; Guillozet-Bongaarts, A.; Ohno, M.; Disterhoft, J.; Van Eldik, L.; Berry, R.; Vassar, R. *J. Neurosci.* **2006**, *26*, 10129.
(28) Mostany, R.; Portera-Cailliau, C. *J. Visualized Exp.* **2008**, e680.
(29) Klunk, W. E.; Bacskai, B. J.; Mathis, C. A.; Kajdasz, S. T.; McLellan, M. E.; Frosch, M. P.; Debnath, M. L.; Holt, D. P.; Wang, Y. M.; Hyman, B. T. *J. Neuropathol. Exp. Neurol.* **2002**, *61*, 797.
(30) Hansen, M. B.; Nielsen, S. E.; Berg, K. *J. Immunol. Methods* **1989**, *119*, 203.



DOI: 10.1021/jacs.5b03548
*J. Am. Chem. Soc.* 2015, 137, 6781−6789